DOE/NV/25946--1976

Linearity for Ca^{2+}-Doped $CeBr_3$ Scintillating Materials

Paul Guss
Principal Investigator

Symposium on Radiation Measurements and Applications (SORMA XV)
June 9–13, 2014

This work was done by National Security Technologies, LLC, under Contract No. DE-AC52-06NA25946
with the U.S. Department of Energy and supported by the Site-Directed Research and Development Program.

Goals

- **Goal:** This project seeks to develop low-cost, high-resolution gamma scintillators based on new fracture-resistant alloys of cerium bromide. These alloys will eliminate limitations imposed by self-activity and fracture of currently available lanthanum-based scintillators.

- **Objectives:**
  (1) Develop low-cost, high-resolution gamma scintillators based on new fracture-resistant alloys of $CeBr_3$.

  (2) Further improve crystals by eliminating radioisotope impurities in the raw materials to enable large, high-sensitivity gamma spectrometers for radioisotope identification and low count rate assay of SNM.

  (3) Demonstrate significant performance advance for applications of importance to DOE missions.

Overview

- Spectroscopy characterization of the crystal delivered by Radiation Monitoring Devices (RMD) to the Remote Sensing Laboratory (RSL).

- Sandia National Laboratories (SNL) mapped out the solid solubility of Ca(II) in $CeBr_3$.

- Pin Yang at SNL determined the material composition by using mass spectrometry techniques (inductively coupled plasma mass spectrometry [ICP-MS]). A comparison of SNL's measured compositions of the RMD fragments was made to assist in characterizing detector performance.

- Pin Yang and Patrick Doty, both of SNL, analyzed the calcium concentrations.

Background

Based on the recent literature on strengthening mechanisms (M. N. Sinha, P. S. Nicholson, “Effect of impurities on the strengthening of CaF_2 single crystals,” *J. Mater. Sci.* **12** (1977) 1451–1462), there are compelling requirements to research and share several ideas, questions, and answers. Sinha and Nicholson’s paper on aliovalent strengthening of CaF_2 attempts to determine mechanisms for low and high temperatures. The authors found that Y(III) gave an order of magnitude greater increase in critical resolve shear stress (CRSS) than Na(I). They conclude the long-range retarding force on dislocations at high temperature is likely due to the induced reorientation of Na(I)/F-vacancy or Y(III)/F-interstitial dipoles in the stress fields of moving dislocations (Snoek effect). This suggested role of the Snoek effect is in accord with analysis of the athermal regime in recent papers on Y-stabilized zirconia and other materials. It then occurs, if the authors are correct, that if anion interstitials balance the charge for the higher-valence cation, then the difference in strength may be related to the higher mobility of interstitials. Interstitial fluoride ion in CaF_2 may be more plausible than interstitial bromide; however, the $CeBr_3$ crystal structure does have large open channels. The SNL team will examine if the M(IV)/Br-interstitial seems like a feasible complex in $CeBr_3$. Since the athermal (high-temperature) regime is probably more important during crystal growth, this work should explore if it makes sense to emphasize M(IV) cations.

SNL

- The amount of calcium in these $CeBr_3$ samples was determined by an induction coupled plasma mass spectrometer. These data will be used to extract the solubility limit.

Figure 1. Packaged scintillator of 1.9% Ca^{2+}-doped $CeBr_3$

Figure 2. Emission spectra

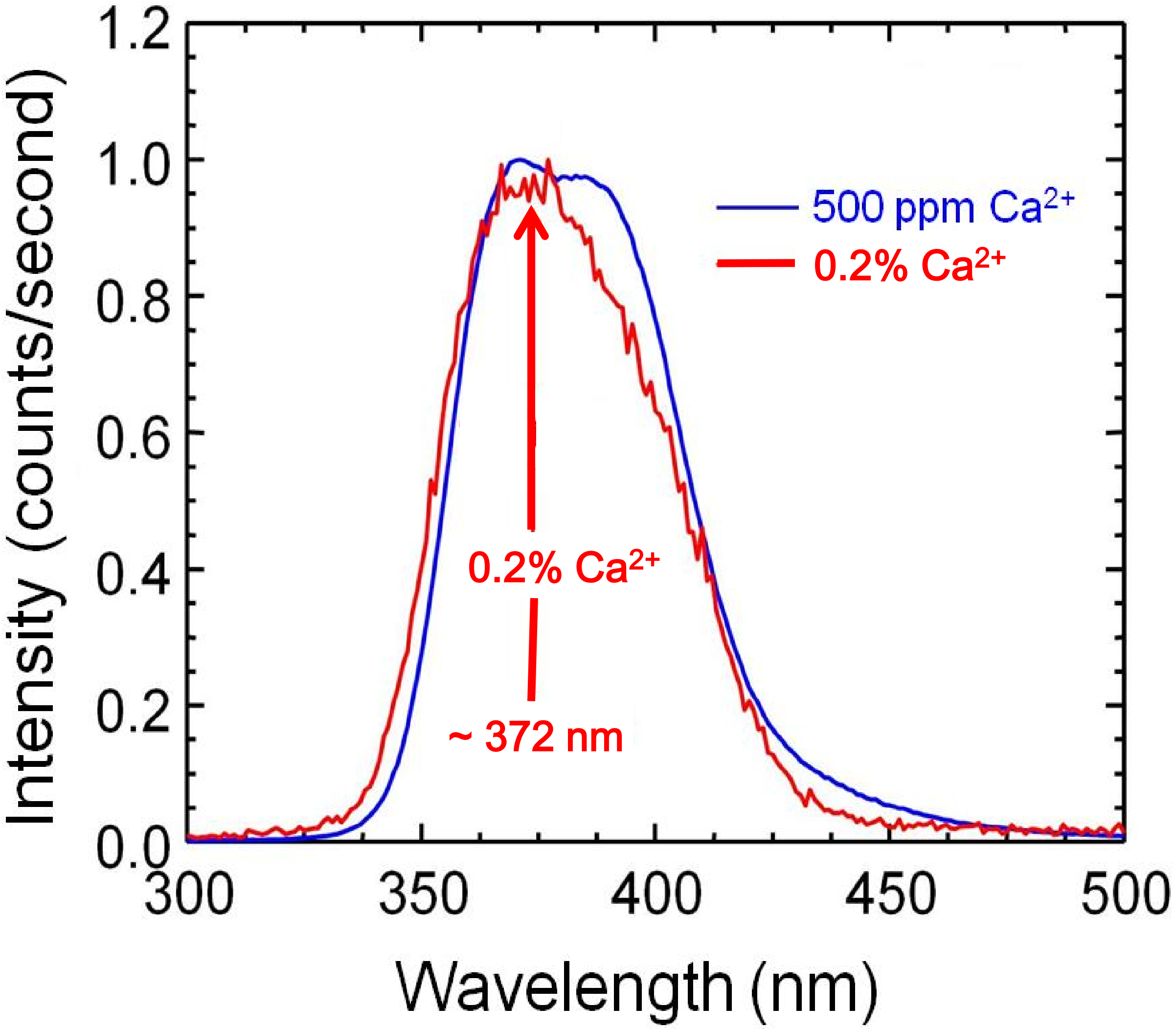

Figure 3. Relative light yield proportionality of Ca^{2+}-doped $CeBr_3$

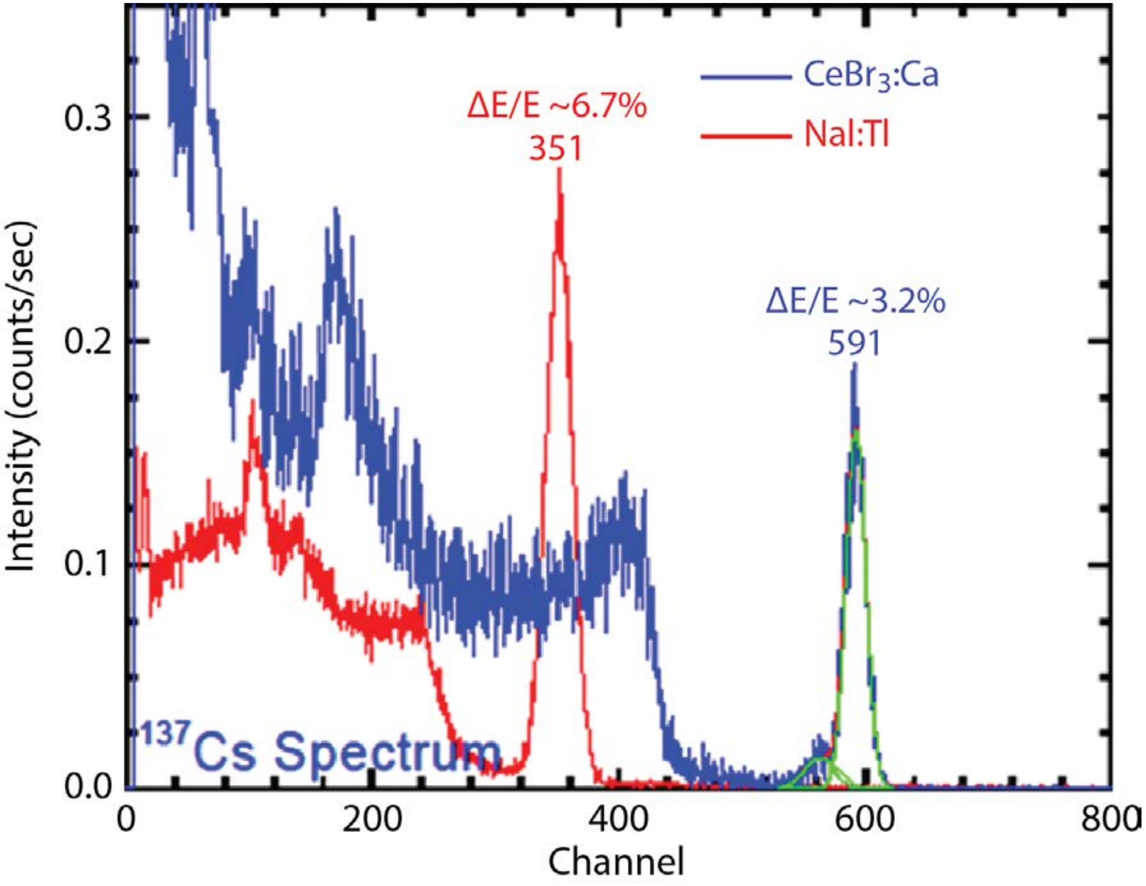

Figure 4. Relative light yield proportionality of Ca^{2+}-doped $CeBr_3$

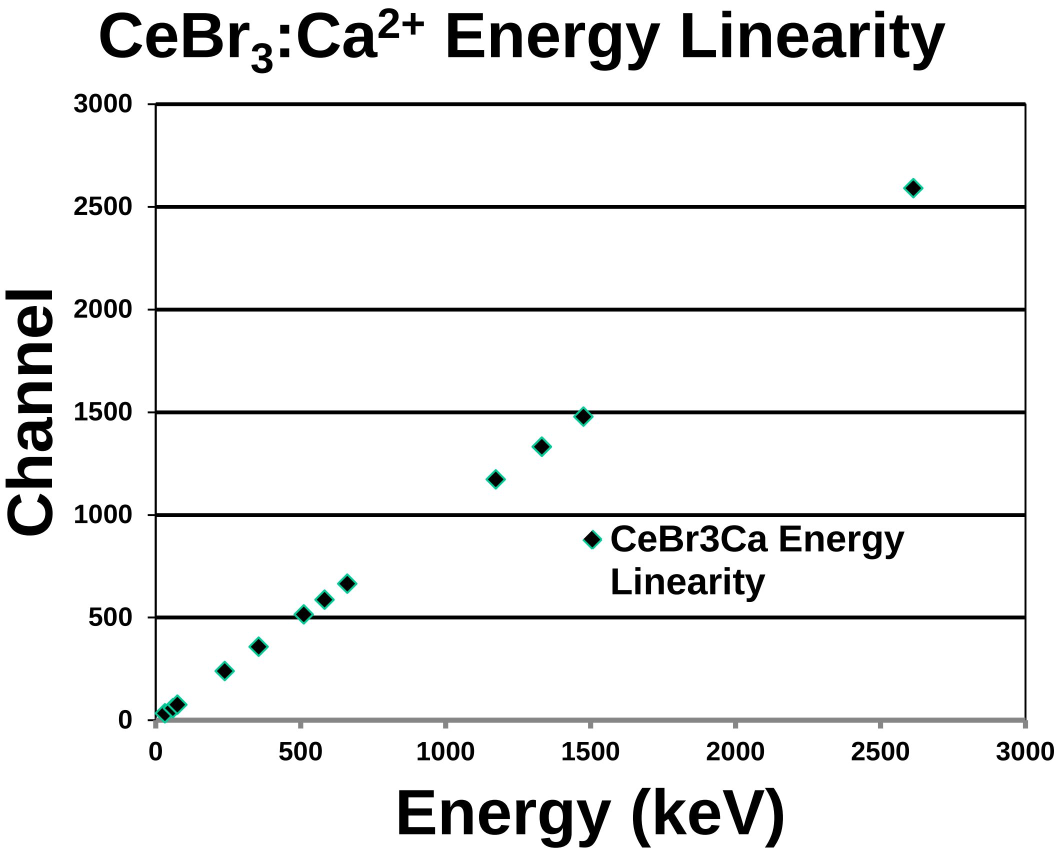

Figure 5. Energy resolution of Ca^{2+}-doped $CeBr_3$

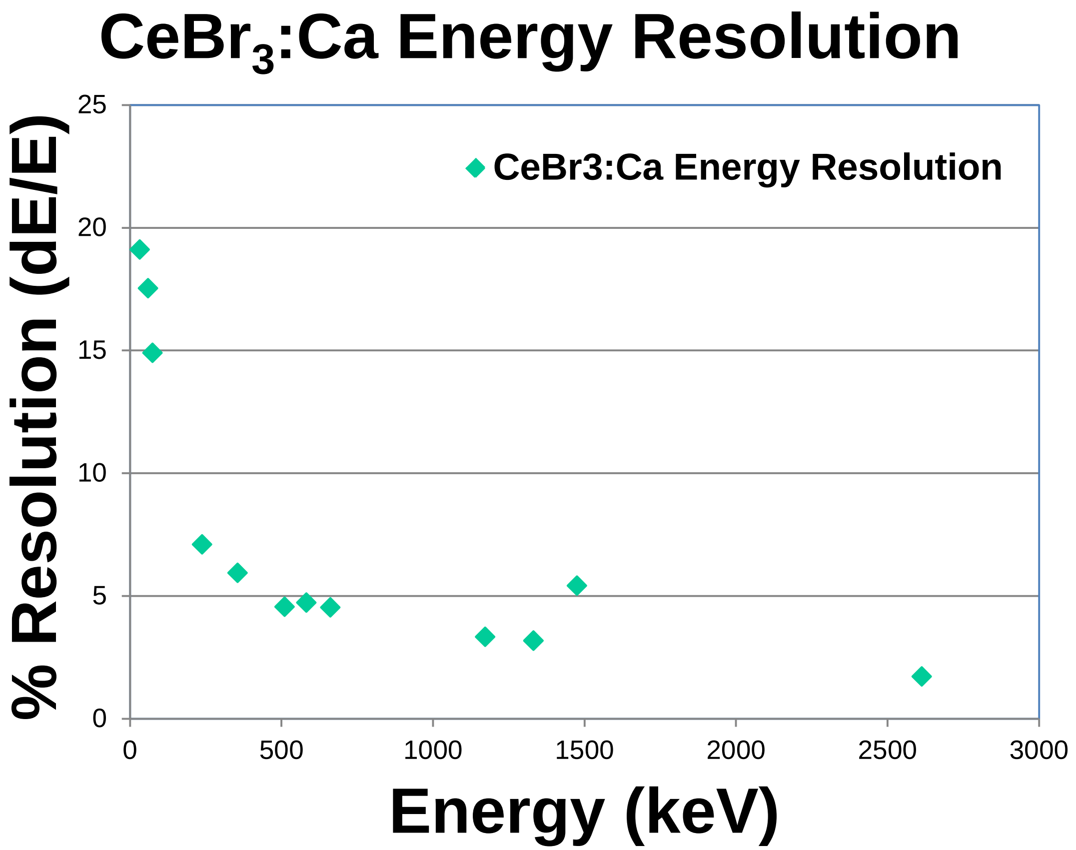

Figure 6. (a) 662 keV spectrum with standard $CeBr_3$ with ~4% FWHM, (b) 662 keV spectrum with $CeBr_3:Ca^{2+}$ with ~3.2% FWHM, (c) improved proportionality for $CeBr_3$:Ca over standard $CeBr_3$

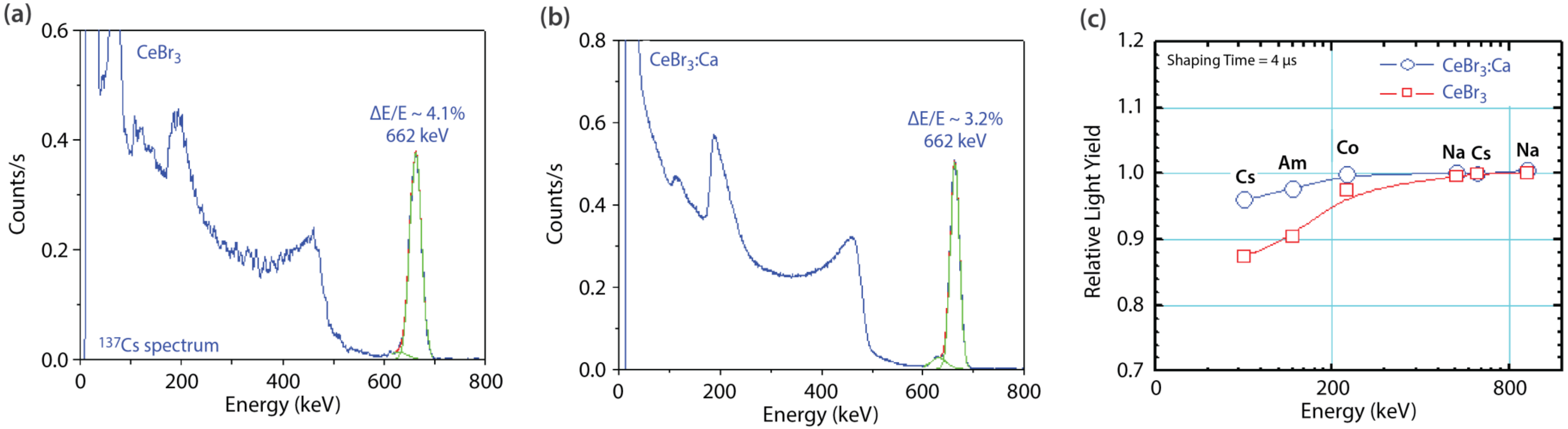

Figure 7. Pulse Shape

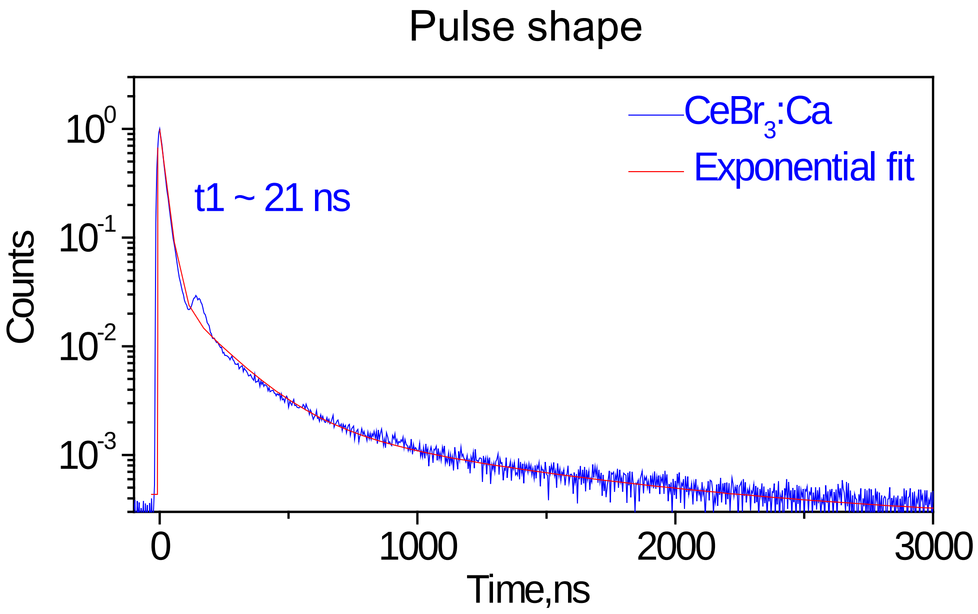

Figure 8. Comparison of measurements with the Ca^{2+}-doped $CeBr_3$ crystal in temporary test can (3.7%) versus the permanent can (4.0%)

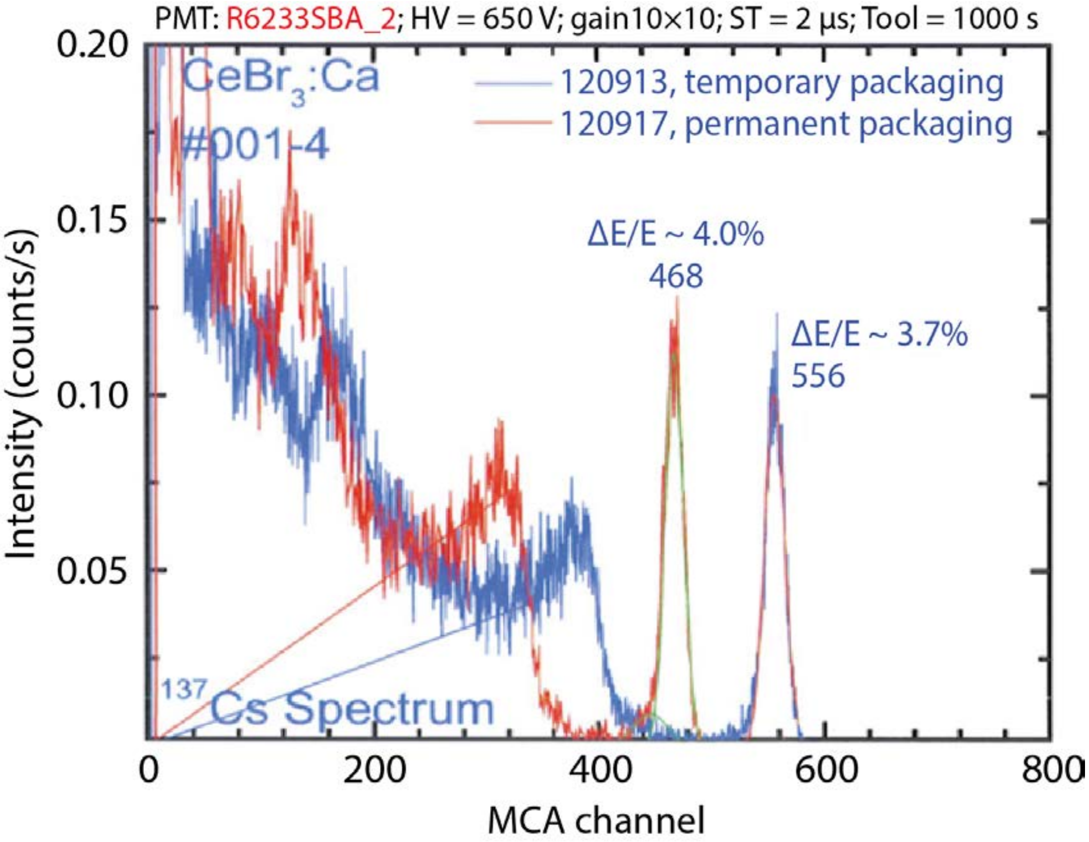

Figure 9. ^{137}Cs Spectrum with the Ca^{2+}-doped CeBr$_3$ crystal in the permanent can (4.5%)

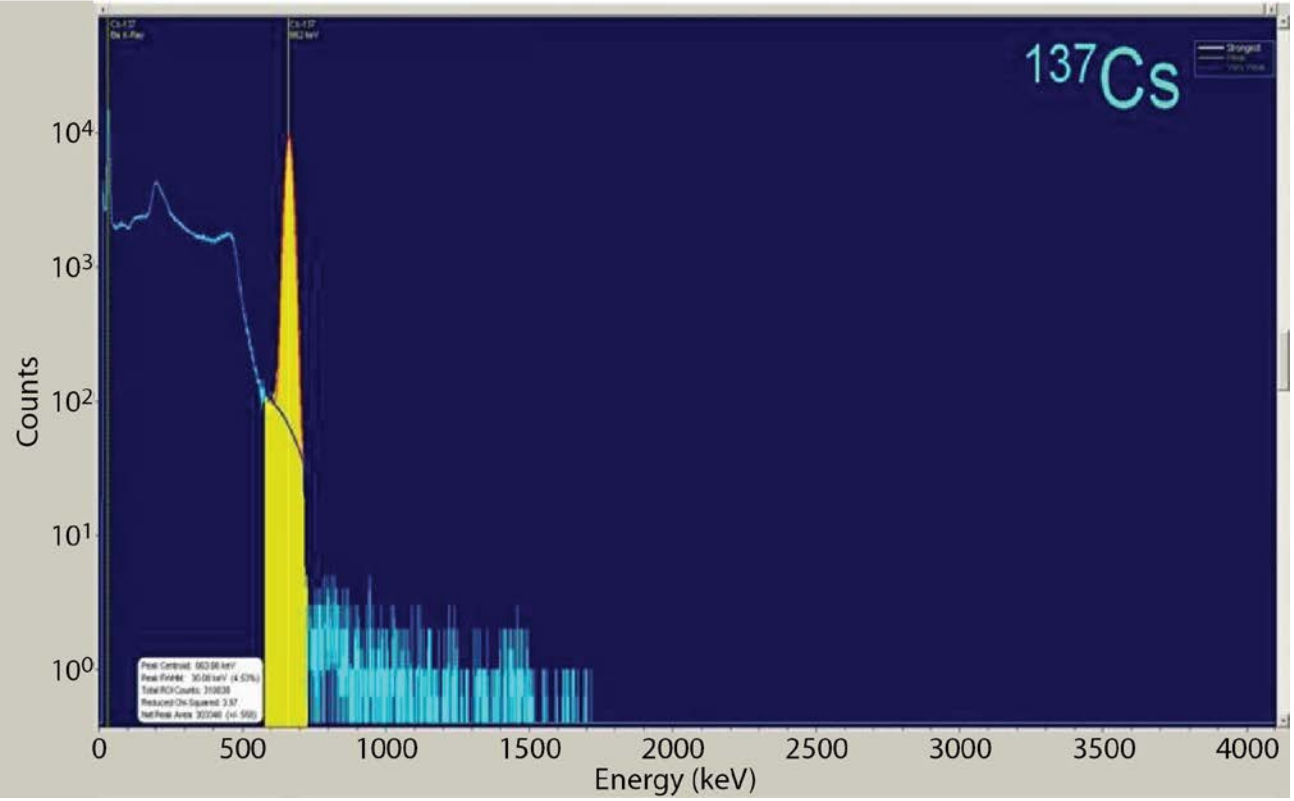

Figure 10. ^{241}Am, ^{60}Co, ^{228}Th, and background spectra with the Ca^{2+}-doped CeBr$_3$ crystal in the permanent can

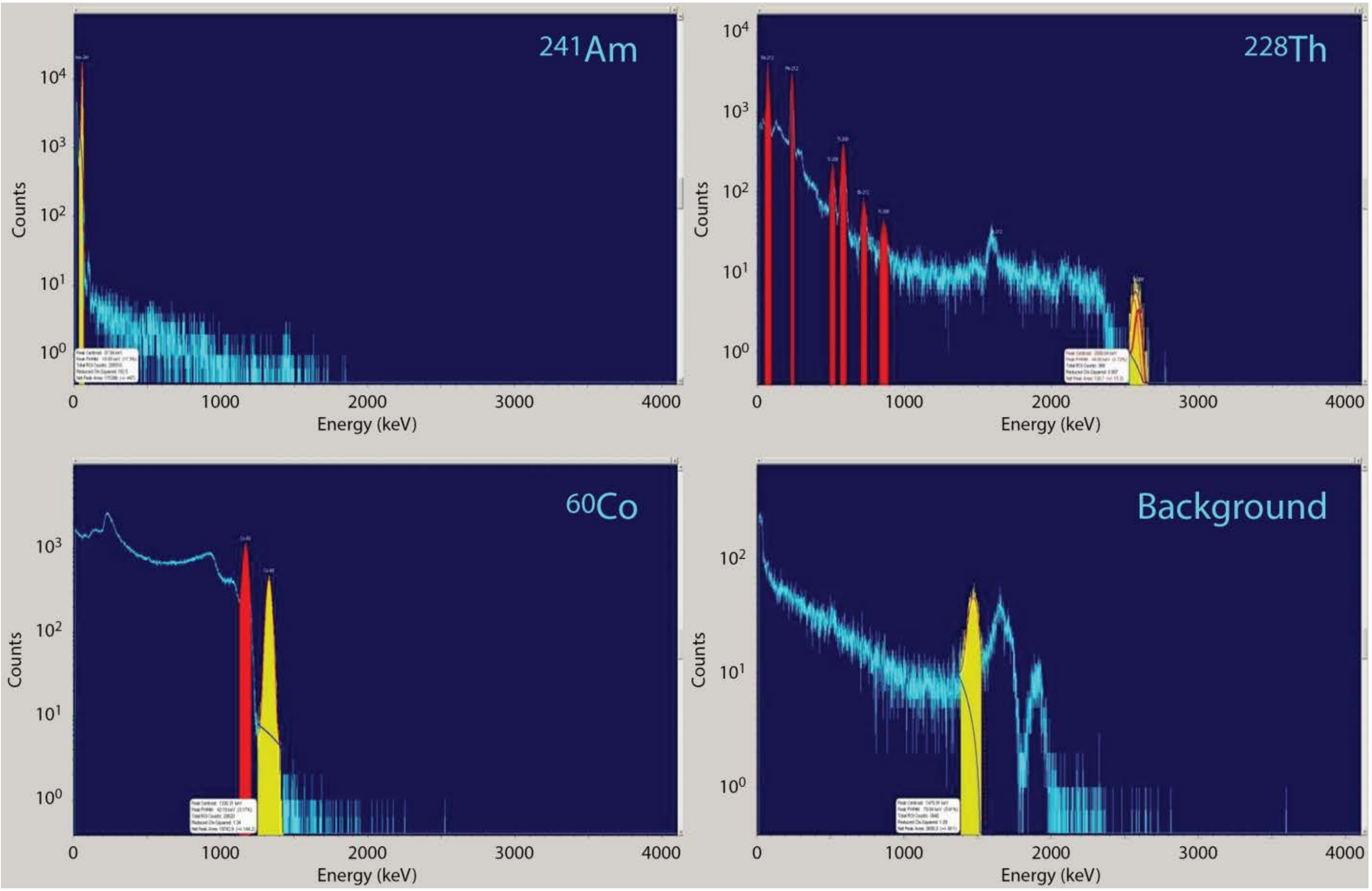

Table 1. Inductively coupled plasma mass spectrometry (ICP-MS) chemical analysis. ICP-MS assays for Ca^{2+}-doped $CeBr_3$; nominal composition 2 wt% $CaBr_2$ in $CeBr_3$

Sample	Calcium Concentration	95% Confidence Limit
#1	0.0238 wt%	0.0014 wt%
#2	0.0212 wt%	0.0015 wt%
#3	0.0192 wt%	0.0015 wt%

Average = 0.0214 ±0.0102 wt.%

Evaluation of Atomic Percentage of Calcium

Atomic % = $40.078x/[(140.116\,(1-x) + 40.078x + 79.904\,(3-x)]$
= 0.00228
= 0.228%

Average calcium weight % concentration,
$x = 0.000214$, in our complex of $Ce_{(1-x)}Ca_xBr_{(3-x)}$,

Atomic % = 0.228 atomic%

Table 2. Differential scanning calorimetric (DCS) results for $CeBr_3$–$CaBr_2$ mixtures in the range 0–10 mole %

Mole % $CaBr_2$	T_m (°C)	T_e (°C)
0	715.3	–
0.2	732.1	–
2.35	721.8	598.3
4.65	715.2	595.4
7.63	706.8	596.2
9.85	697.3	597.0

The mixtures show linear trends, including an apparent eutectic temperature $\mathbf{T_e}$ near 597°C for calcium concentrations ≥2.35%.

Figure 11. Phase diagram for $CeBr_3$–$CaBr_2$

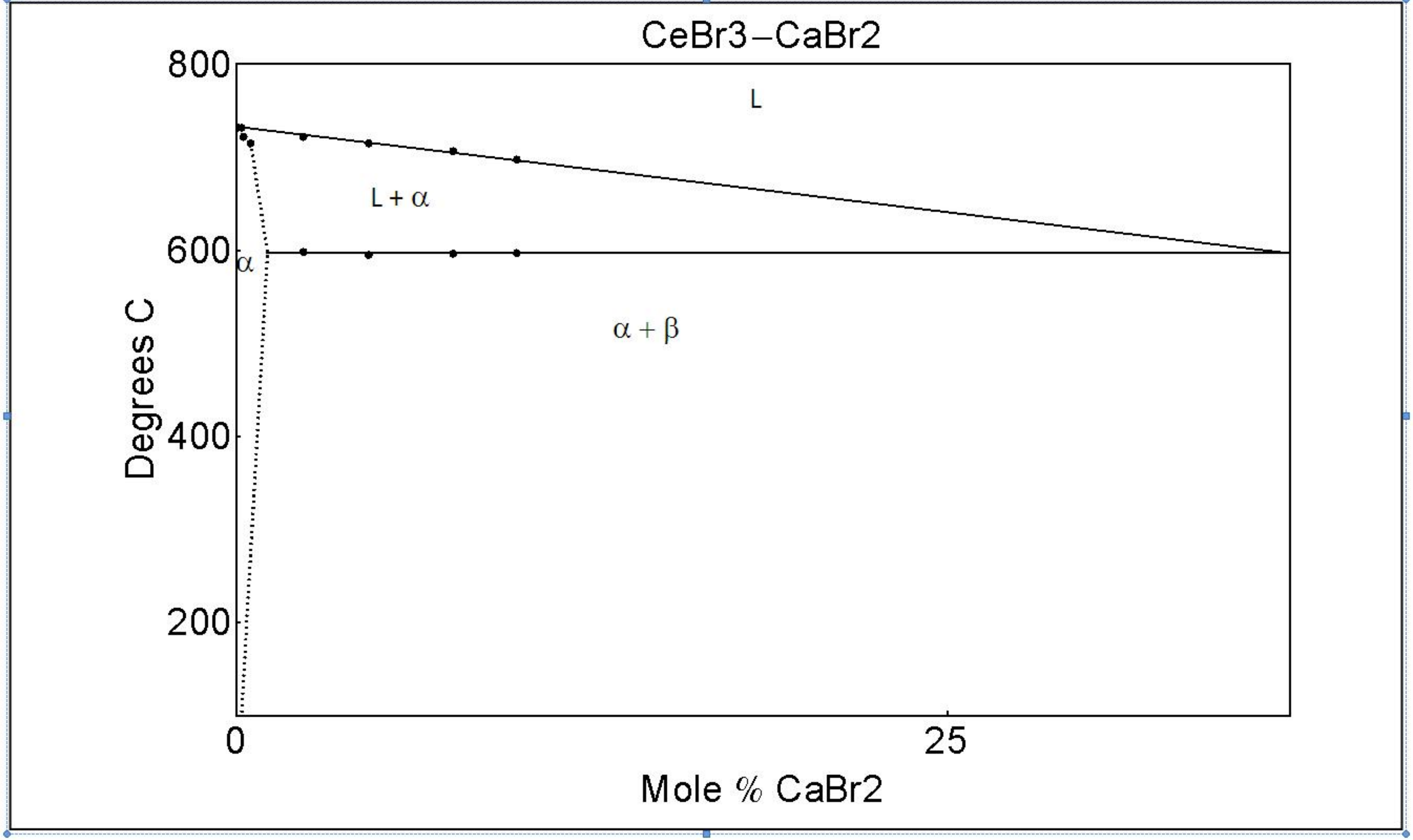

Table 3. Measured total light yield data; calculated and estimated total light yield

Material	Peak FWHM (%)	Est. Total Light Yield (ph/MeV)	Reference
$CeBr_3$	5.6	68,000	Guss
$CeBr_3$ + 0.2% $CaBr_2$	3.2	62,000	Guss
$CeBr_3$ + 500 ppm $CaBr_2$	4.5	65,200	RMD 2009
BGO	10	8,200	Harrison
$CeBr_3$ + 500 ppm $SrBr_2$	4.9	48,600	Harrison
$CeBr_3$ + 500 ppm $CdBr_2$	6.7	34,800	Harrison
$CeBr_3$ + 500 ppm $ZrBr_4$	6.6	37,600	Harrison
$CeBr_3$ + 1000 ppm $HfBr_4$	5	52,900	Harrison
$LaBr_3$ + 5% $CeBr_3$	4.2	85,100	Harrison
NaI:Tl	8.3	36,700	Harrison

Technical Issues

- Need to determine concentration of calcium. If it cracks at saturation, may not determine accurate concentration.
- Need to benchmark below solubility limit.
- Need to examine other dopants, such as Ba, Sr, and Cd (SDRD project convincingly eliminated Pb).

Future Direction

- Complete analysis of spectroscopy benchmarking
- Calculate with a less dilute doping (i.e., something less than 2%) of Ca in $CeBr_3$. This will help with the assessment what doping concentration will lead to changes in optical and mechanical properties.
- Perform hardness measurements to see if the aliovalent approach hardened the crystal as expected
- Other reasonable research areas include:
    - Calculate density functional theory (DFT) model with less-dilute doping
    - Perform growth with lower concentrations of calcium
    - Perform similar growth runs using strontium

Summary

- New DFT simulations demonstrate a capability for predicting properties of doped $CeBr_3$ materials that is unavailable elsewhere but is critically needed to study the property-limiting valence phenomena in ionic compounds
- Assessed concentrations and the solubility limit
- RSL benchmarked the Ca^{2+}-doped $CeBr_3$ crystal
- The Ca^{2+}-doped $CeBr_3$ crystal has improved energy resolution (i.e., 3.2%)
- The Ca^{2+}-doped $CeBr_3$ crystal has improved linearity over the pure $CeBr_3$ crystal

Acknowledgments

Bryan Wong (SNL) performed the DFT calculations.

Patrick Doty (SNL) provided advice and guidance.

RMD prepared the crystal and performed some of the characterization.

Marlene Bencomo (UNM) assisted with IC-PMS analysis.

The author also thanks Thomas Stampahar, Michael Lukens, John O'Donoghue, Michael Mohar, and Sanjoy Mukhopadhyay of NSTec for their contributions to this work.

References

[1] Shah, $CeBr_3$ Scintillators for Gamma-Ray Spectroscopy DOE Contract No. DE-AC03-76SF00098, RMD.
[2] Guss, NIM A **608**, 2 (2009) 297.
[3] Guss, SPIE **7805** (2010) L-1.
[4] Shah, IEEE Trans. Nucl. Sci., **51**, no. 5 (2004) 2395–2399.
[5] Doty, Proc. Mat. Res. Soc. **1038** (2008) 1-8.
[6] Harrison, SPIE **7806** (2010) M-1.
[7] Pletka, Physica Status Solidi **39** (1977) 301–311.
[8] Setyawan, Wahyu; Curtarolo, Stefano. "High-throughput electronic band structure calculations: Challenges and tools." Comp. Mat. Sci. **49**: (2010) 299–312.
[9] Li, Chenliang, Biao Wang, Rui Wang, Hai Wang. “First-principles studies on the electronic and optical properties of $CeCl_3$ and $CeBr_3$.” Solid State Communications 144 (2007) 220–224.
[10] Periodic Table of the Elements: LANL. http://periodic.lanl.gov/list.shtml (accessed February 6, 2012).
[11] Snoek, J., “Effect of small quantities of carbon and nitrogen on the elastic and plastic properties of iron,” *Physica* **8**, 7 (1941) 711–733.
[12] Sinha, M. N., P. S. Nicholson, “Effect of impurities on the strengthening of CaF_2 single crystals,” *J. Mater. Sci.* **12**, 7 (1977) 1451–1462.
[13] Hall, R. N., “Variation of the distribution coefficient and solid solubility with temperature,” *J. Phys. Chem. Solids* **3**, 1–2 (1957) 63–73.
[14] Fischler, S., “Correlation between maximum solid solubility and distribution coefficient for impurities in Ge and Si,” *J. Appl. Phys.* **33**, 4 (1962) 1615.
[15] P. Guss, et al., *Site-Directed Research and Development*, FY 2013, National Security Technologies, LLC, Las Vegas, Nevada, 2014.